Nie *et al.*
Journal of Engineering and Applied Science (2023) 70:45
https://doi.org/10.1186/s44147-023-00217-5

Journal of Engineering and Applied Science

RESEARCH **Open Access**

Study on anti-crack effect of semi-rigid base pavement with stress absorbing layer

Dan Nie[1], Shuxia Wang[2], Panxu Sun[3*] and Changjing Huang[1]

*Correspondence:
panxusun@zzu.edu.cn

[1] School of Urban and Rural Architectural, Minxi Vocational and Technical College, Longyan 364021, China
[2] School of Materials Science and Engineering, Zhengzhou University of Aeronautics, Zhengzhou 450046, China
[3] School of Civil Engineering, Zhengzhou University, Zhengzhou 450001, China

Abstract

For the characteristics of semi-rigid base asphalt pavement prone to cracking, various stress-absorption layers are applied widely by decreasing stress concentration, improving interlayer bonding and waterproofing. Existing studies on the anti-cracking effect of stress absorbing layers rarely consider top-down fatigue cracking on the outside of the boundary of the vehicle loading zone. Firstly, this paper proposes a finite element model setting a downward expansion of fatigue crack in pavement based on fracture mechanics. The influence law of modulus and thickness of stress absorbing layer on stress intensity factor of crack tip and the fatigue life of the pavement is analyzed furthermore. Numerical calculation results demonstrate that shearing stress intensity factor increases with stress absorbing layer thickness and decreases with stress absorbing layer modulus, while fatigue life of pavement grows with the modulus of the stress absorbing layer and decreases with its thickness. Sensitivity analysis indicates that the modulus of the stress absorbing layer has a greater effect on the fatigue life of the pavement relative to thickness, which offers reference for further promotion and application of stress absorbing layer.

Keywords: Stress absorbing layer, Fatigue crack, Stress intensity factor, Asphalt pavement, Fatigue life

Introduction

Semi-rigid base asphalt pavement is peculiarly prone to cracks under the action of temperature, humidity, and repeated traffic loads. The circumstances for crack growth and the elements influencing it include a number of aspects, and asphalt pavement cracking can take many distinct shapes in practice. Ameri et al. [1] and Sun et al. [2] both studied top-down cracking in the transverse direction under traffic loading, while Kang et al. [3] comparatively studied longitudinal top-down cracks and base reflective cracks that run transversely. By various modeling methods used in numerical simulation, combining dynamic modulus test and bending test, many scholars have devoted themselves to studying the fracture mechanics, crack paths, propagation phase and fracturing modes of pavement cracks [4–6]. The existence and expansion of cracks will not only affect the driving comfort of the road, reduce the durability of the road, but also even trigger the destruction of the entire pavement structure. The study mentioned above demonstrates that the evaluation index based on fracture mechanics is in line with the functioning state of semi-rigid subgrade pavement with cracks. As a material with some initial defects in general, it is trustworthy to apply the fracture mechanics theory to analyze the cracking issue of asphalt pavement.

On that basis, a technology that can reduce and retard the occurrence and development of cracks in semi-rigid base asphalt pavements was proposed. By absorbing stress concentration in the crack portion and enhancing interlayer bonding and waterproofing, the setting of stress-absorbing layer can vastly ameliorate the cracking problem of semi-rigid base asphalt pavement. Normal placement of the stress-absorbing layer is between the asphalt surface and the semi-rigid base or between the asphalt surface and the old cement concrete panel. From the earliest Strata stress absorbing layer developed by Koch company in the USA, geogrids, geotextiles, modified asphalt geogrids, and modified asphalt are a few of the stress-absorbing layers that have been created over the past 50 years [7–9]. The issue of cracking has not been fully solved by any of these methods yet because some performed poorly when put under a variety of field situations [10].

Several tests have verified the effectiveness and applicability of the anti-cracking properties of certain stress absorbing layers. Pan et al. [11] noted that warm mix rubber modified asphalt mixture was ideal for using as a stress absorbing layer to prevent road cracking in cold regions. Yang, et al. [12] analyzed the anti-crack performance of enhanced stress absorbing layer when slow cracking based on fatigue crack propagation tests. Sun et al. [13] compared the crack resistances of high viscous asphalt sand stress-absorption layer, common SBS modified asphalt stress absorbing layer and rubber asphalt stress-absorption layer. The ability of the stress absorbing layer to slow down the crack expansion depends on the kind of stress absorbing layer and external conditions. The former includes additive types, stiffness, and thickness, the latter is mainly load level and temperature [14, 15]. Han et al. [16] discussed the effects of modulus, thickness, and porosity of stress absorbing layer between the old concrete pavement and asphalt pavement on the stress by numerical simulation. Based on the response surface methodology, Nejad et al. [17] investigated the effect of temperature, crack width, geosynthetic type (polypropylene nonwoven and glass grid), and interactions between these parameters on reflective crack propagation were analyzed.

Currently, there are relatively mature works on how to install a stress absorbing layer under asphalt concrete overlay on top of existing cement concrete slab, but the impact of placing it directly between the base and the surface layer is still unclear. Additionally, most international studies on how a stress absorbing layer affects crack expansion have been conducted on reflection cracks [18, 19]. The traditional asphalt pavement design method considers that the fatigue effect of tensile stress at the bottom of each structural layer is the primary cause of structural layer cracking. Bottom cracks extend to the surface of the pavement leading to fatigue cracking of the surface. However, the downward expansion of fatigue cracks in semi-rigid base asphalt pavements is also one of the sources of damage to the pavement structure [20]. The tensile stresses and strains on the outer side of the load area boundary will damage the asphalt surface and cause top-down fatigue cracking of the road surface. Applied to resist reflection cracks, the stress absorbing layer is directly contact with the initial crack and can play a direct function in the upward expansion of reflection cracks. In contrast, the stress absorbing layer is not directly contact with the top-down preliminary crack. Its indirect effect may be quite different. Therefore, it is necessary to analyze the contribution of stress absorbing layer to the top-down preliminary crack in the asphalt structure.

In this paper, the top-down expansion of fatigue cracks in semi-rigid base asphalt pavements with stress absorbing layer is analyzed. In "Methods" section, the fracture mechanics theory of fatigue cracks is introduced. In "Results and discussion" section, a numerical model of semi-rigid subgrade pavement with cracks is established using fracture mechanics theory. The influence law of modulus and thickness of stress absorbing layer on stress intensity factor of crack tip and fatigue life of pavement is analyzed and the top-down expansion law of fatigue cracks is studied in "Conclusions" section. The findings can further provide theoretical support and technical guidance for the further promotion and application of composite pavement.

Methods

Fracture mechanics and Paris formula

Cracks are classified into three different types in fracture mechanics based on the stress condition in the cracks: opening mode, shearing mode and tearing mode, as shown in Fig. 1.

The unified formula that can be used to express the stress and displacement fields at the crack tips of the three different types is [22]

$$\begin{cases} \sigma_{ij}^{(N)} = \dfrac{K_N}{\sqrt{2\pi r}} f_{ij}^{(N)}(\theta) \\ \mathrm{u}_i^{(N)} = K_N \sqrt{\dfrac{r}{\pi}} g_i^{(N)}(\theta) \end{cases} (i,j = 1,2,3) \tag{1}$$

where σ_{ij} $(i,j = 1,2,3)$ is the stress component; $u_i (i = 1,2,3)$ is the displacement component; $K_N(N = \mathrm{I,II,III})$ is the stress intensity factor (SIF) and $N = \mathrm{I,II,III}$ denotes the type of crack; $f_{ij}(\theta)$ and $g_i(\theta)$ are both functions of the polar angle θ; r is the distance to the crack tip.

Equation (1) exhibits the following properties of stress field at crack tip. First above all, the stress field features a singularity that the stress at the crack tip is indefinitely high ($r=0$). Secondly, the stress is directly proportional to the parameter K_N. As long as K_N is the same, the stress field at the tip will be completely consistent. Evidently, the crack tip stress field singularity is stronger and the probability that the crack would be unstable increases with the stress intensity factor. So, based on the aforementioned properties of the fracture tip stress field, the stress intensity factor $K_N(N = \mathrm{I,II,III})$, which is used

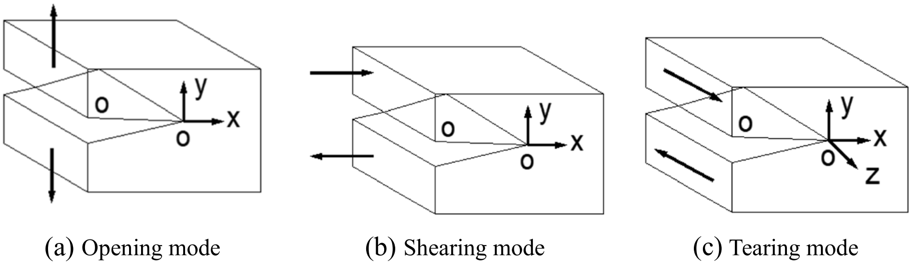

(a) Opening mode (b) Shearing mode (c) Tearing mode

Fig. 1 Three types of cracks [21]. **a** Opening mode. **b** Shearing mode. **c** Tearing mode

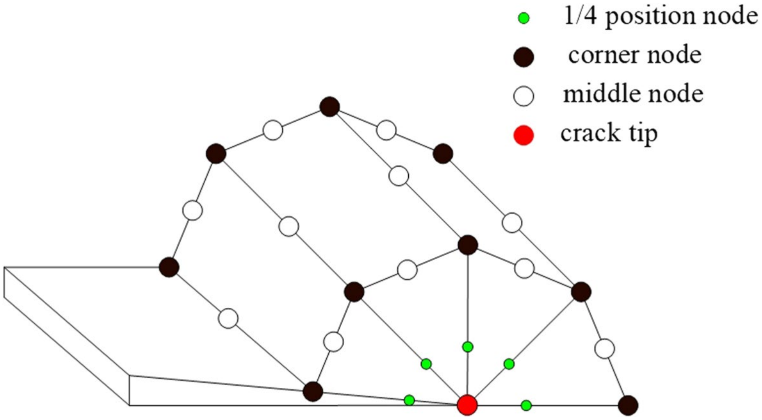

Fig. 2 Singular element types and nodes around crack tip

to describe the strength of the stress field at the tip of three different types of cracks, is defined by fracture mechanics as Eq. (2) illustrated:

$$\begin{aligned} K_{\mathrm{I}} &= \lim_{r\to 0}\sqrt{2\pi r}\sigma_y(r,0) \\ K_{\mathrm{II}} &= \lim_{r\to 0}\sqrt{2\pi r}\tau_{xy}(r,0) \\ K_{\mathrm{III}} &= \lim_{r\to 0}\sqrt{2\pi r}\tau_{yz}(r,0) \end{aligned} \tag{2}$$

where σ_y is the y-axis normal stress; τ_{xy} is the shear stress in xoy plane; τ_{yz} is the shear stress in yoz plane.

The displacement method and the stress method, which compute the SIF value using the nodal displacement or stress close to the crack tip, are two commonly employed direct methods for calculating the stress intensity factor. The displacement approach frequently produces results that are more accurate than those of the stress method because the stress field is generated by the partial derivative of the displacement field. As shown in Fig. 2, the crack tip can acquire singularity by simply shifting the middle node of the 20-node isoparametric element to the 1/4 position to make it a degenerative singular element [23, 24]. Thus, the displacement of the node at the crack tip point and 1/4 position may be used to calculate the stress intensity factor, and the equations for the three different types of stress intensity factors can be provided as follows:

$$\begin{aligned} K_{\mathrm{I}} &= \frac{2\mu}{\kappa+1}\sqrt{\frac{2\pi}{r_{a-b}}}(v_b - v_a) \\ K_{\mathrm{II}} &= \frac{2\mu}{\kappa+1}\sqrt{\frac{2\pi}{r_{a-b}}}(u_b - u_a) \\ K_{\mathrm{III}} &= \mu\sqrt{\frac{\pi}{2r_{a-b}}}(w_b - w_a) \end{aligned} \tag{3}$$

where κ is the material parameter related to Young's modulus and Poisson's ratio; μ is the shear modulus; r_{a-b} is the distance between crack tip node and 1/4 node; u_a and u_b are the x-direction displacements of the tip node and 1/4 position node of the crack front, respectively; v_a and v_b are the y-direction displacements of the tip node and 1/4 position node of the crack front, respectively; w_a and w_b are the z-direction displacements of the tip node and 1/4 position node of the crack front, respectively. Note that all displacements here are in the local Cartesian coordinate system.

Unlike the stress intensity factor, which can only characterize the ease of crack expansion, the Paris formula can be used to describe the crack opening and expansion process. If the external load acts cyclically N times and the crack expands as a, then the crack expands as *a/N* for each cycle of the crack. Paris formula considers the fatigue expansion rate of the crack under repeated loading $\mathrm{d}c/\mathrm{d}N$ as a function of the increase in SIF as shown in Eq. 4 [25].

$$\mathrm{d}c/\mathrm{d}N = A(\Delta K)^n \tag{4}$$

Further integration gives the number of load actions:

$$N_f = \int_{c_0}^{c_f} \frac{\mathrm{d}c}{A(\Delta K)^n} \tag{5}$$

where $\mathrm{d}c/\mathrm{d}N$ is the crack expansion rate; c_0 and c_f are the initial crack size and the final crack size respectively; $\Delta K = K_{\max} - K_{\min}$ is the increase of the stress intensity factor; A and n are constants related to the material properties, which is usually determined by conducting fatigue experiments.

The applicability of fracture mechanics principles in predicting the fatigue life of pavements has been confirmed through extensive theoretical analysis and experimental research. It is proved that the development of cracks in asphalt mixes is in accordance with the crack expansion law established by Paris, and the theory of fatigue fracture mechanics can be utilized to forecast the fatigue life of asphalt mixtures [26, 27]. After the stress absorbing layer is added to the road, most of the cracks are still located in the asphalt surface layer and the theory above can still be applied. As a result, SIF will be used as a characterization index for the development of cracks. And it's also the basis to investigate the effect on the fatigue life of semi-rigid subgrade pavements when the stress absorbing layer's parameter changes in the following part.

Based on fracture mechanics and Paris formula, the numerical simulation of anti-crack effect of semi-rigid base pavement with stress absorbing layer can be realized, and the corresponding flow chart is shown in Fig. 3. The whole process consists of four steps. Firstly, the finite element software ANSYS is used to establish the road structure model with crack on the surface of asphalt pavement. By aid of the comparison of the analysis without stress-absorbing layer, the correctness of the numerical simulation method is verified. Secondly, the effect of stress absorbing layer thickness and modulus on SIF is studied. Thirdly, the impact of stress absorbing layer on fatigue life is investigated by curve fitting and Paris formula. Lastly, sensitivity analysis of the effect of modulus and thickness is realized.

Basic assumption

The hypotheses are that each layer of road structure is composed of homogeneous, elastic and isotropic materials. Layers are in constant interaction with one another. The

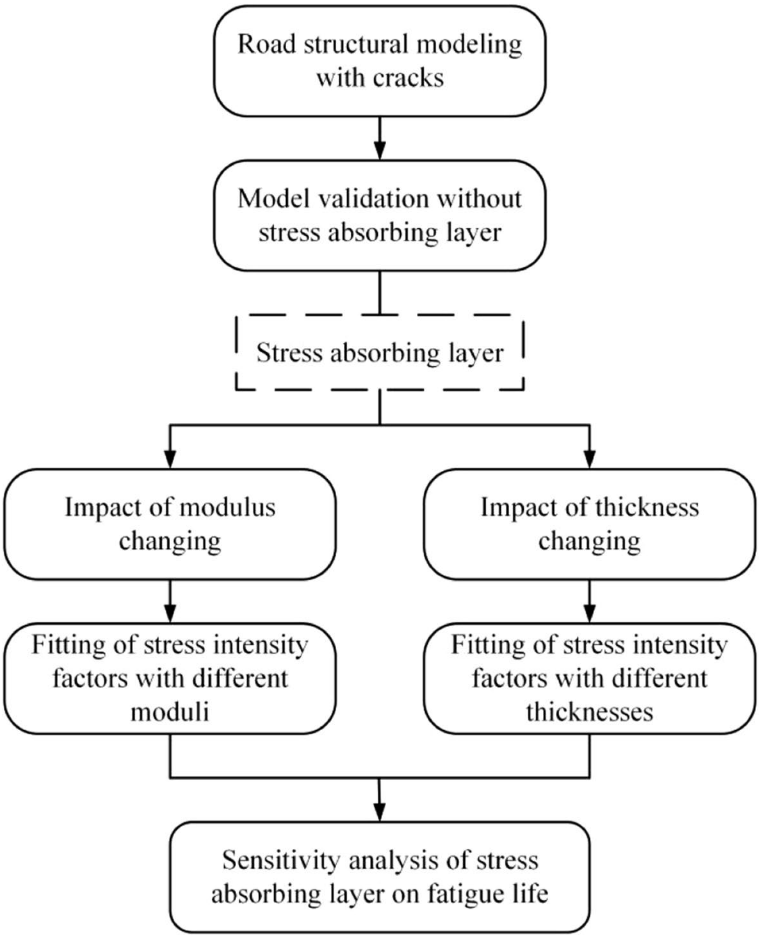

Fig. 3 The flow chart of numerical simulation

horizontal and downward dimensions of the soil base are assumed to be infinite. Furthermore, cracks only extend downward in the vertical direction.

The most unfavorable load

It is proved that the stress intensity factor at the pavement crack's tip keeps a negative value under symmetric load, which means that the two faces of the crack move in opposite directions of extrusion and the crack can hardly expand in this case [28]. Therefore, only asymmetric load will be applied on the model with transverse cracks. When the vehicle is moving, the location of the asymmetric loading is obtained based on the maximum probability of occurrence [29], as shown in Fig. 4. It will also be the main reason for the expansion of pavement cracks. According to the current Chinese specification, it is assumed in this paper the tire contact width B is 18.8 cm, the center distance between two wheels is 31.8 cm and the contact length L is 19.0 cm as shown in Fig. 4.

Road structure

A typical representative road structure was adopted with its thickness and material parameters listed in Table 1. The road structure consists of asphalt surface layer, stress absorbing layer, cement stabilized macadam semi-rigid base and roadbed, where the

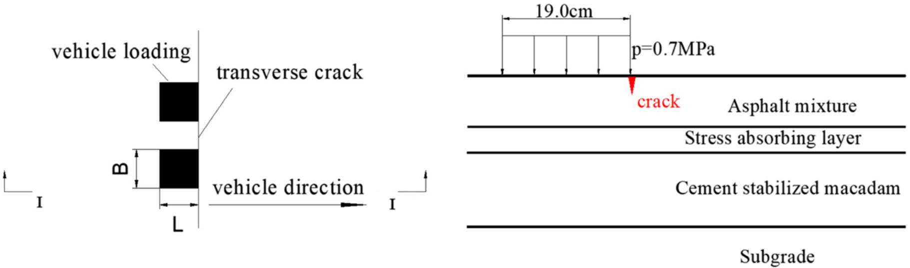

(a) The most unfavorable load of transverse crack

(b) I-I cross section diagram

Fig. 4 Diagram of cracks. **a** The most unfavorable load of transverse crack. **b** I-I cross section diagram

Table 1 Parameters of the road structure

Basic structure	Thickness/m	Modulus/MPa	Density/kg/m^3	Poisson's ratio
Asphalt mixture	0.18	10,622	2400	0.35
Rubber asphalt stress absorbing layer (with or without)	0.01–0.05	2000–6000	2500	0.30
Cement stabilized macadam	0.36	1300	2300	0.25
Subgrade	7	60	1800	0.45

stress absorbing layer is temporarily not set in the model validation but set in the actual analysis. Asphalt pavement is usually designed based on elastic layer system theory, using Young's modulus of elasticity as a basic mechanical parameter for calculation. The mechanical parameter for asphalt surface layer and stress absorbing layer can be determined by reference [30], and static modulus is used for semi-rigid subgrade and road base referring to the recommended practice of AASHTO 2002.

As a multi-layered structure, the stress intensity factor will change abruptly between layers so that the cracking and transmission mechanism between layers will be significantly complicated with the increase of pavement layers. To further facilitate in finite element calculation, top surface course, intermediate layer, and the following layer are simplified into a unified layer based on the modulus and Poisson's ratio conversion equations derived from the membrane force equivalence in Eq. 6 and Eq. 7 [31]. The thickness of top layer is 0.04 m, the thickness of middle layer is 0.06 m, and the thickness of bottom layer is 0.08 m. The asphalt mixture is converted into one layer. The equivalent modulus is 10622 MPa and the total thickness remains 0.18 m.

The Poisson ratio of the equivalent structure is expressed as

$$v = \frac{\sum_{i=1}^{n} \frac{E_i h_i v_i}{1-v_i^2}}{\sum_{i=1}^{n} \frac{E_i h_i}{1-v_i^2}} \tag{6}$$

The modulus of the equivalent structure is expressed as

$$E = \frac{1-\nu}{h}\sum_{i=1}^{n}\frac{E_i h_i}{1-\nu_i} \tag{7}$$

where h is the total thickness of structural layers;E_i, h_i, and ν_i are respectively modulus, thickness and Poisson's ratio of the ith layer.

Finite element modeling

As shown in Fig. 5, ANSYS APDL is used to produce a finite element model of preinstalled fractures on the top of an asphalt mixture to investigate the top-down cracks propagation rule based on the theory of linear elastic fracture mechanics. This is a 3D model employing solid45 and solid95 elements. Since the crack is only hypothesized to develop downward (in the vertical direction), it is only modeled in the crack length region. Secondly, the downward expansion of road cracks under vertical vehicle loads is an example of in-plane stressing in fracture mechanics. It means the probability of cracks breaking along the length direction is very small and K_{III} is usually not considered [32, 33]. So a thin model is adopted.

The beginning depth of the crack is fixed at 0.007 m since initial cracks are frequently present before operation [34]. The model width is taken as 10 m, and the thickness of the roadbed is taken as 7 m. The direct modeling method is employed in this bottom-up modeling starting from the crack front to provide better control of the cell accuracy especially in the area close to the crack. As stated in the previous section, it is required to set the first cell at the crack tip as Singular elements to describe its singularity of the stress and strain field when modeling. A macro program offsets the center nodes of the isoparametric cells surrounding the original tip by 1/4 to produce three-dimensional singular elements automatically while Solid45 solid elements are used in other area. To increase calculation accuracy, the transitional elements are placed close to the full crack model tip. The computational model of the road is large in size. However, the crack size is small, which is as low as 10^{-3} m in one dimension. In the XOY plane, i.e., the vertical section of the road, the edge length of singular elements is always kept 0.01 times of the crack depth for calculation. The tip model is composed of 16 singular pieces to

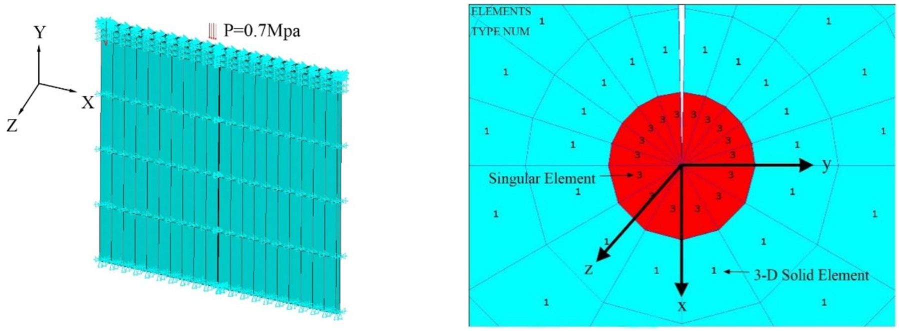

(a) Finite element meshing and loading in global coordinate system

(b) Elements type number and local coordinate system

Fig. 5 Finite element model and grid layout. **a** Finite element meshing and loading in global coordinate system. **b** Elements type number and local coordinate system make sure that there is no less than one element within 30°. The crack length direction is defined as being along the *Z*-axis direction and the depth direction is defined as the *Y*-axis direction under the global coordinate system. Depending on the basic assumptions above, the cracks only extend along the *Y*-axis direction.

The boundary conditions of the model simulate how the road structure is actually constrained. Complete restraint is applied to the bottom surface of the soil base and no displacement is allowed. The *X*-axis displacement is limited in the road cross-sectional direction, while the *Z*-axis displacement is limited in the road's length direction. The pavement's surface serves as a free surface for the application of axle load. Vertical displacement is allowed besides the bottom surface of the structure.

Results and discussion

Model validation

The static load method is the most commonly used method to calculate the fatigue life [1, 32]. Therefore, the static load method is used to calculate the stress intensity factor. The nodes displacement of crack tip can be obtained by aid of the post-processing of ANSYS. Then SIF can be directly calculated based on Eq. (3). For the sake of comparing, the stress intensity factor of crack tip in the model without stress absorbing layer is calculated. The thickness of asphalt mixture surface layer is 0.18 m. The thickness of rigid base layer is 0.36 m. But the stress absorbing layer is not installed [29]. The road parameters listed in Table 1 are exactly the same as those of the road model in the literature. The loading in the literature is consistent with Fig. 4. The tire contact width is 18.8 cm, the center distance between two wheels is 31.8 cm and the contact length is 19.0 cm. When the crack length is 0.12 mm and the modulus of cement stabilized macadam base varies from 500 to 6000 MPa as shown in Fig. 6, the simulation results show considerable consistency with the data of the reference. The relative errors of the calculations are within 5% and the accuracy of the modeling and calculation techniques used in this study is proved. A snapshot of the von Mises stress distribution map at the crack tip is shown in Fig. 7. Obviously, the stress value increases as one gets closer to the fracture tip, which on the other hand proves the effectiveness of singular elements.

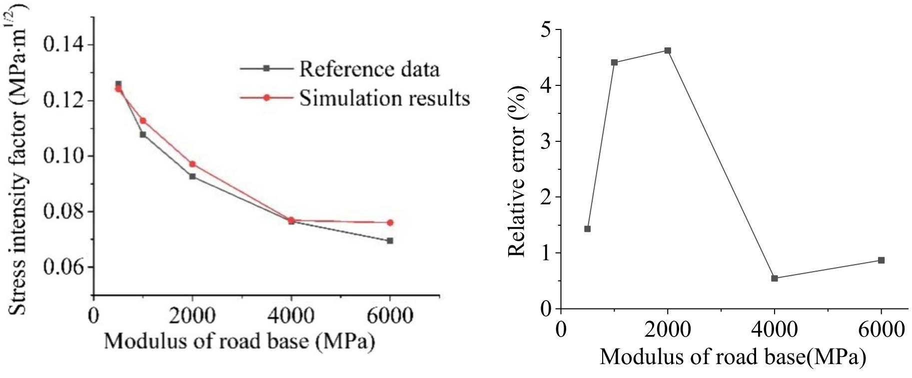

(a) Comparison of stress intensity factor (b) Relative error

Fig. 6 Comparison of simulation results with reference data. **a** Comparison of stress intensity factor. **b** Relative error

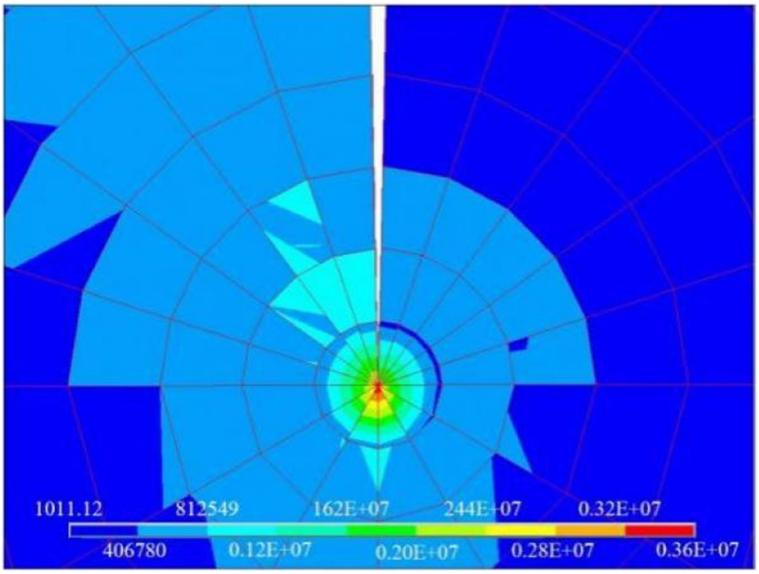

Fig. 7 Von Mises stress distribution map at the crack tip

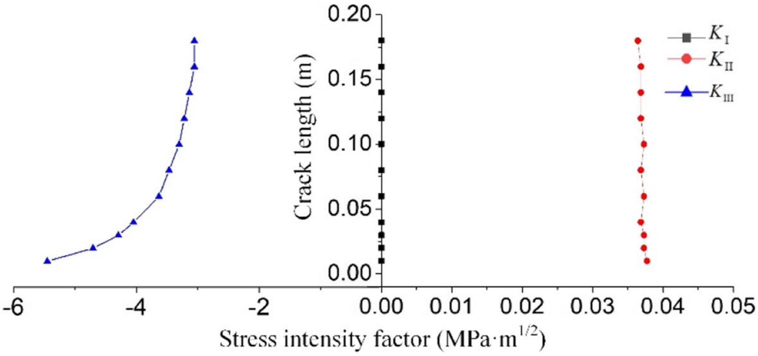

Fig. 8 The variation of SIF with crack length

Effect of stress absorbing layer on stress intensity factor

The road structure is re-modeled and re-computed in the same way based on the road structure added a stress absorbing layer shown in Fig. 4, intending to research how SIFs change when stress absorbing layer modulus and thickness vary. When the modulus of stress absorber layer is 4000 MPa and its thickness is 0.05 m. The depth of crack is 0.03 m. The stress intensity factors of cracks with varying crack length are displayed using quadrant graphs with scatter plots in Fig. 8. Figure 9 shows the SIFs with various depths of cracks. When the length of crack is 0.01 m, the modulus of the stress absorbing layer is 4000 MPa and the thickness of the stress absorber layer is 0.05 cm. Combining these two pictures, it reveals that K_{III} (tearing type) is always negative while K_{I} (opening type) maintains 0 regardless of changes in the length and height of the crack. This means that the probability of crack opening in the XOY plane under asymmetrical load as well as shearing along the *Z*-axis is 0, which is consistent with the basic assumptions proposed previously. As a result, K_{II} is the topic of discussion below.

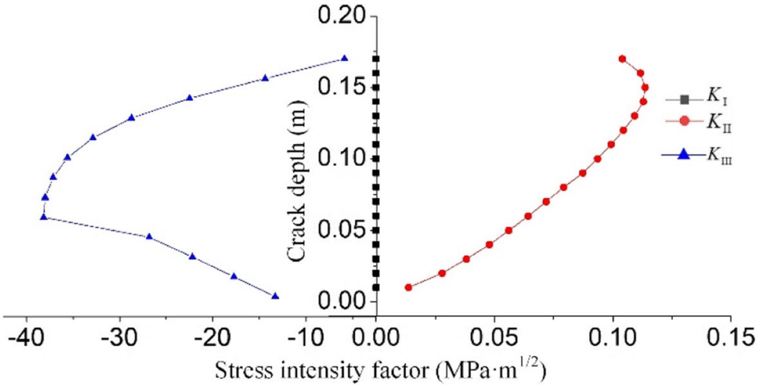

Fig. 9 The variation of SIF with crack depth

Figure 10 shows that K_{II} at the crack tip basically steps down as the crack length grows. On the contrary, K_{II} becomes clearly larger as the crack depth becomes larger shown in Fig. 11. The likelihood that a fracture may become unstable and enlarge grows as the crack's depth rises. As all the four graphs illustrated, K_{II} increases with stress absorbing layer thickness and decreases with stress absorbing layer modulus, which is less obvious

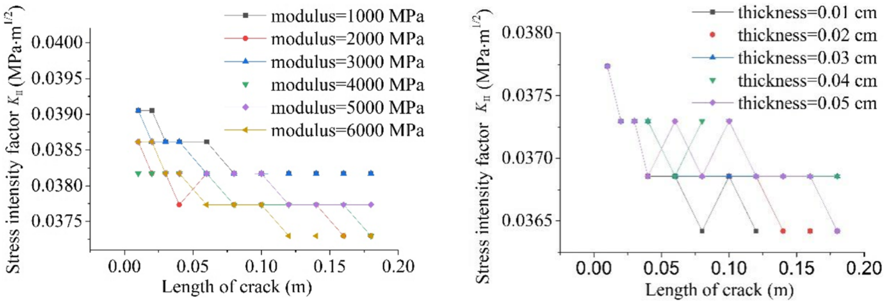

(a) The variation of K_{II} with the crack length in different modulus

(b) The variation of K_{II} with the crack length in different thickness

Fig. 10 The variation of KII with the crack length. **a** The variation of KII with the crack length in different modulus. **b** The variation of KII with the crack length in different thickness

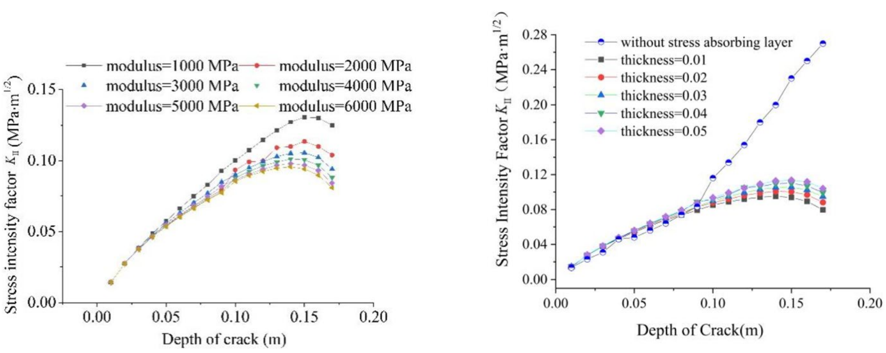

(a) The variation of K_{II} with the crack depth in different modulus

(b) The variation of K_{II} with the crack depth in different thickness

Fig. 11 The variation of KII with the crack depth. **a** The variation of KII with the crack depth in different modulus. **b** The variation of KII with the crack depth in different thickness in the pictures of Fig. 10 but clearer in Fig. 11. The variation pattern of K_{II} with increasing crack depth is also shown in Fig. 11b for the road structure without stress absorbing layer. When the stress-absorbing layer has been laid, the stress intensity factors at the crack tips are all lower.

Effect of stress absorbing layer on fatigue life

To clarify how the parameters of the stress absorbing layer actually affect the fatigue life of pavement, the SIFs are factored as a function of crack length and depth using the polynomial form, which is stated in the Eq. (8).

$$K_{\mathrm{II}} = p_1 h_{\mathrm{d}}^4 + p_2 h_{\mathrm{d}}^3 + p_3 h_{\mathrm{d}}^2 + p_4 h_{\mathrm{d}} + p_5 \tag{8}$$

where p_1, p_2, p_3, p_4, and p_5 are polynomial coefficients obtained by fitting, h_{d} is the depth of crack, K_{II} is the shearing stress intensity factor.

When taking into account the possibility of crack expansion in the length and depth directions, the function fitting is utilized based on Fig. 11. The pavement service life can be obtained by first substituting the fitted function expression into the Paris formula and then integrating it over the range of crack depth variation. Since no experiments were conducted, the parameters A and n in the Paris equation used in this paper were obtained by referring to the reference [29], taking $A = 1.72 \times 10^{-5}$ and $n = 1.60$. Figure 12 depicts the influence of the stress-absorbing layer's modulus and thickness on fatigue life. The diagram shows that in the specified range, the crack fatigue propagation life grows with the modulus of the stress absorbing layer and decreases with its thickness. Similarly, the SIFs at the crack tip without stress absorbing layer in Fig. 11b are also fitted to the depth to further calculate the fatigue life. The fatigue life of the pavement without a stress absorbing layer, with other structural layers of the pavement having the same parameters, is 0.14×10^6. Obviously, regardless of the parameters chosen, installing a stress absorbing layer between the semi-rigid base and the asphalt surface layer significantly improves the fatigue life of the pavement. Its setting is beneficial to retard the top-down expansion of fatigue cracks on the road surface. However, it should be noted that in order to obtain better crack relief, an excessively thick stress absorbing

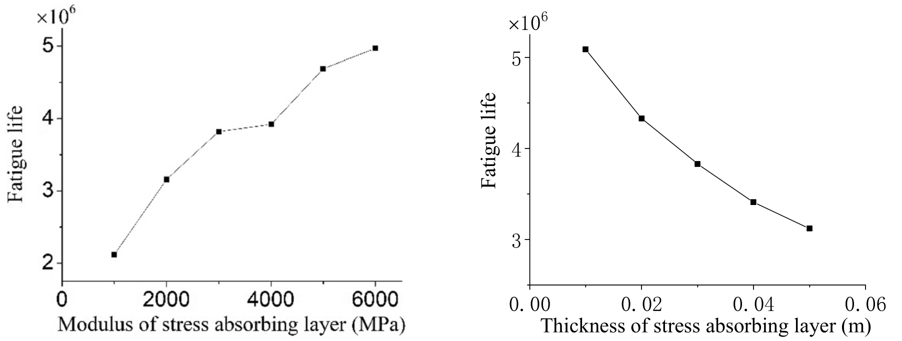

(a) The variation of fatigue life with modulus (b) The variation of fatigue life with thickness

Fig. 12 The variation of fatigue life. **a** The variation of fatigue life with modulus. **b** The variation of fatigue life with thickness layer should not be installed. Besides, the recalculated fatigue life is 0.14×10^6 and it is lower than the fatigue life from Fig. 12b assuming the thickness is 0. The main reason for this phenomenon is that the model is valid only for a certain thickness interval. The thickness of stress absorbing layer is usually larger than 0.01 m in practical engineering. The proposed calculated model based on polynomial function is only applicable to the stress absorbing layer with thickness greater than 0.01 m. A new model has to be investigated, which could be applicable in the case of thin stress absorbing layers.

When the crack is located between the semi-rigid base and stress absorbing layer, the effectiveness of preventing reflection crack increases with the decrease of the modulus of the stress absorbing layer [35]. However, the law of the top-down expansion of fatigue crack that located in asphalt structure is different. As the modulus of the stress absorbing layer increases, the stress of crack tip decreases and the fatigue life increases.

Equation (9) defines the sensitivity factor that can be used to evaluate the effect magnitude of the thickness and modulus of the stress absorbing layer on fatigue crack extension.

$$S_{AF} = \frac{\Delta A/A}{\Delta F/F} \tag{9}$$

where S_{AF} is the sensitivity factor; $\Delta F/F$ is the rate of change of the factor F; $\Delta A/A$ is the rate of change of fatigue life as an evaluation indicator when the uncertainty factor F changes by ΔF. The sensitivity of the modulus of the stress absorbing layer to fatigue life is 0.269 based on Eq. (9). The sensitivity of the thickness of the stress absorbing layer to fatigue life is − 0.096. It indicates that the modulus of the stress absorbing layer has a greater effect on the fatigue life of the pavement relative to thickness.

Conclusions

The effect of stress absorbing layer's setting on the fatigue life of semi-rigid base asphalt pavement with initial cracks is analyzed. The top-down expansion of the near-surface cracks at the boundary of the wheel-loaded area within the asphalt surface layer is taken as the source of damage. A numerical model of road with cracks with stress intensity factor as the evaluation index is established based on fracture mechanics in this paper. The accuracy of the numerical calculation approach based on finite elements is confirmed. Some conclusions are as follows:

(1) The effect of stress absorbing layer on stress intensity factor is analyzed. The numerical results show that SIFs of the K_{III} type (opening type) is negative while K_{I} maintains 0, K_{II} becomes clearly larger as the crack depth becomes larger. Besides, K_{II} increases with stress absorbing layer thickness and decreases with stress absorbing layer modulus.

(2) The effect of the stress absorbing layer on fatigue life is analyzed. The results show that with increase of the modulus of stress absorbing layer, the fatigue life increases gradually. With increase of the thickness of stress absorbing layer, the fatigue life decreases gradually. Based on sensitivity analysis, the modulus of the stress absorbing layer has a greater effect on the fatigue life of the pavement relative to thickness.

There are still some limitations in this study. In future work, the anti-crack effect of semi-rigid base asphalt pavement with stress absorbing layer under the temperature and load frequency will be conducted.

Abbreviation

SIF	Stress intensity factor

Acknowledgements
Not applicable

Authors' contributions
DN was the major contributor in writing the manuscript. SW conducted the visualization and comparison. PS conducted the conceptualization, formal analysis and writing—review. CH provided some data. The authors read and approved the final manuscript.

Funding
This research was funded by the Education and Scientific Research Project for Middle-aged and Young Teachers in Fujian Province (Grant No. JAT191532), Research on Vocational Education Teaching Reform of Longyan City (Grant No. ZJKT2022004), Science and Technology Research Project of Henan Province (Grant No. 222102230010) and Key Research Project of Henan Higher Education Institutions (Grant No. 22A560005).

Availability of data and materials
The datasets used and/or analyzed during the current study are available from the corresponding author on reasonable request.

Declarations

Competing interests
The authors declare that they have no competing interests.

Received: 16 February 2023 Accepted: 7 May 2023

References

1. Ameri M, Mansourian A, Khavas MH, Aliha MRM, Ayatollahi MR (2011) Cracked asphalt pavement under traffic loading-a 3D finite element analysis. Eng Fract Mech 78(8):1817–1826
2. Sun L, Duan Y (2013) Dynamic response of top-down cracked asphalt concrete pavement under a half-sinusoidal impact load. Acta Mech 224:1865–1877
3. Kang Z, Guannan Y, Jianfeng L, Linbing W (2021) Study on fracture characteristics of asphalt pavement with longitudinal and transverse cracks under the influence of real temperature field. IOP Conf Ser: Earth Environ Sci 719:032072
4. Yuan R, Zhao L (2022) Viscoelastic-thermodynamic model and crack propagation in asphalt concrete pavement. Secur Commun Netw 2022:6603130
5. Xu Y, Jiang Y, Xue J, Ren J (2019) Investigating the effect of aggregate characteristics on the macroscopic and microscopic fracture mechanisms of asphalt concrete at low-temperature. Materials 12(17):2675
6. Ruan L, Luo R, Zhang D, Wang B (2021) Numerical simulation of crack paths in asphalt mixture using ordinary state-based peridynamics. Mater Struct 54:1–19
7. Dempsey BJ, Mukhtar, MTSDM (1996) Stress absorbing composite for road repair. US, US5513925 A.
8. Komatsu T, Kikuta H, Tuji Y, Muramatsu E (1998) Durability assessment of geogrid-reinforced asphalt concrete. Geotext Geomembranes 16(5):257–271
9. Ogundipe OM, Thom N, Collop A (2013) Investigation of crack resistance potential of stress absorbing membrane interlayers (SAMIs) under traffic loading. Constr Build Mater 38:658–666
10. Dempsey BJ (2002) Development and Performance of Interlayer Stress-Absorbing Composite in Asphalt Concrete Overlays. Transp Res Rec 1809(1):175–183
11. Pan R, Li Y (2020) Effect of warm mix rubber modified asphalt mixture as stress absorbing layer on anti-crack performance in cold region. Constr Build Mater 251:118985
12. Yang S, Li P, Guo M, Liao S, Wu H (2020) Study on dynamic load monitoring of an enhanced stress absorption layer. Front Mater 7:148
13. Sun Y, Yan T, Wu C, Sun X, Wang J, Yuan X (2018) Analysis of the fatigue crack propagation process of the stress-absorption layer of composite pavement based on reliability. Appl Sci-Basel 8(11):2093
14. Zeng Z, Guo Y, Li P, Shen A, Zhai C (2021) Performance research of fiber-reinforced asphalt rubber as a stress-absorbing membrane interlayer. J Adhes Sci Technol 35(19):2047–2063
15. Shafabakhsh G, Ahmadi S (2021) Reflective cracking reduction by a comparison between modifying asphalt overlay and sand asphalt interlayer: an experimental evaluation. Int J Pavement Eng 22(2):192–200
16. Han L, Zhang S, Zhang Z, Gao T (2022) Mechanical analysis of preventing reflection cracks based on stress absorbing layer. Adv Civ Eng 2022:8016215

17. Nejad FM, Asadi S, Fallah S, Vadood M (2016) Statistical-experimental study of geosynthetics performance on reflection cracking phenomenon. Geotext Geomembranes 44(2):178–187
18. Hao Z, Liu J, Chang J (2020) Study on the effect of HDPE stress absorbing layer in preventing reflective cracks. In Proceedings of the Transportation Soil Engineering in Cold Regions, Singapore, 331–341.
19. Wang H, Wu Y, Yang J, Wang H (2021) Numerical simulation on reflective cracking behavior of asphalt pavement. Appl Sci-Basel 11(17):7990
20. Zheng J (2014) New structure design of durable asphalt pavement based on life increment. China J Highw Transp 27(1):1–7
21. Williams ML (1957) On the stress distribution at the base of a stationary crack. J Appl Mech 24:109–114
22. Irwin GR (1957) Analysis of stresses and strains near the end of a crack traversing a plate. J Appl Mech 24:361–364
23. Henshell RD, Shaw KG (1975) Crack tip finite elements are unnecessary. Int J Numer Methods Eng 9(3):496–507
24. Barsoum RS (1976) On the use of isoparametric finite elements in linear fracture mechanics. Int J Numer Methods Eng 10(1):25–37
25. Paris P, Erdogan F (1963) A Critical analysis of crack propagation laws. J Basic Eng 85:528–533
26. Christensen RM, Wu EM (1981) A theory of crack growth in viscoelastic materials. Eng Fract Mech 14(1):215–225
27. Seo Y, Kim YR, Schapery RA, Witczak MW, Bonaquist RA (2004) Study of crack-tip deformation and crack growth in asphalt concrete using fracture mechanics. In Proceedings of the Technical Sessions of the Journal of the Association of Asphalt Paving Technologists. Baton Rouge, Louisiana, 697–730.
28. Yuan S, Tan Z (2007) Analysis of fatigue fracture on vertical reflective crack under traffic load on asphalt pavement. J Tongji Univ Nat Sci 35(10):1352–1357
29. Luan L (2017) Research on fatigue crack propagation and fatigue life prediction of semi-rigid base asphalt pavement. China Civ Eng J 50(9):118–128
30. Bari J, Witczak MW (2006) Development of a new revised version of the Witczak E Predictive Model for hot mix asphalt mixtures. Road Mater Pavement 75:381–423
31. Wu HL (1997) Discussion on the effective elastic moduli in the unsymmetrical multi-layer plate. J Geomech 3(2):24–32
32. Ziari H, Aliha MRM, Mojaradi B, Sarbijan MJ (2019) Investigating the effects of loading, mechanical properties and layers geometry on fatigue life of asphalt pavements. Fatigue Fract Eng Mater Struct 42(7):1563–1577
33. Aliha MRM, Ziari H, Mojaradi B, Sarbijan Jebalbarezi M (2020) Modes I and II stress intensity factors of semi-circular bend specimen computed for two-phase aggregate/mastic asphalt mixtures. Theor Appl Fract Mec 106:102437
34. Tutu KA, Timm DH (2022) Recursive pseudo fatigue cracking damage model for asphalt pavements. Int j Pavement Eng 23(8):2654–2674
35. Wang X, Zhong Y (2019) Influence of tack coat on reflective cracking propagation in semi-rigid base asphalt pavement. Eng Fract Mech 213:172–181

Publisher’s Note